RADIAL VIBRATION ANALYSIS OF BEARINGLESS SLICE MOTORS

Herbert Grabner, Hartmut Bremer, Wolfgang Amrhein, Siegfried Silber

LCM - Linz Center of Competence in Mechatronics
Johannes Kepler University Linz
A-4040 Linz, Austria
herbert.grabner@lcm.at

ABSTRACT

The bearingless slice motor with PM excited two pole rotor naturally shows a non-linear force distribution. It is common to use standard PID-position-controllers for industrial applications, hence it is important to know how linear control schemes will be influenced by the non-linear part.

Thus, this paper is concerned with rotordynamic phenomena caused by linearly controlled bearingless slice motors. The eigenvalues of the equation of motion illustrate a region of rotational speed, at which instability occurs. It is shown that with an appropriate value of damping established by the controller or by the surrounding medium asymptotical stability can be achieved. Furthermore, the effect of applying arbitrary disturbance forces and the effect of static unbalance are treated and the maximum stationary radial amplitudes of the centre of mass are pictured. Finally, the possible benefits of a complex non-linear controller design will be discussed.

INTRODUCTION

During the past decade there have been some significant advances in the areas of bearingless motor technology. Over the years, the first serial products entered the market and it turned out that compared to usual motor bearing concepts, this kind of technology entails a lot of advantages. Bearingless drives need no lubrication, they have almost unlimited lifetime and they can be used in several applications where demands on cleanness, chemical resistance and tightness are important [1],[2]. However, mechanical and electrical complexity is high and therefore in the range of low cost applications they hardly gain ground.

A very simple mechanical design can be achieved with a bearingless slice motor with PM excited rotor [3]. An advantage of this drive configuration is that only the radial position and the rotor angle need to be controlled actively. Axial position of the rotor as well as tilting is stabilized passively by means of magnetic reluctance forces [4]. That's why, an active engagement can hardly be realised and vibrations excited in these degrees of freedom are not addressed in the proposed approach.

Several applications entail different process forces which act on the rotor and thus radial position controllers must be able to handle all of them. Engineers are used to implement PID-controllers because they are well known and of high robustness, but do they meet the requirements of any application? To answer this question, the next sections show an approach of the bearingless slice motor from a rotordynamic point of view.

MATHEMATICAL MODEL

Description of the Model

Particularly, for high-speed applications the PM rotor features one polepair with almost sinusoidal field distribution to keep the motor losses to a minimum.

However, in this arrangement any radial displacement causes magnetic forces as well as coupling of magnetic forces in x- and y-direction depending on the rotor angle γ

$$\mathbf{F}_{mag} = k_x \begin{bmatrix} 1 + c_x \cos(2\gamma) & c_x \sin(2\gamma) \\ c_x \sin(2\gamma) & 1 - c_x \cos(2\gamma) \end{bmatrix} \begin{bmatrix} x \\ y \end{bmatrix},$$

with k_x denoting the natural negative stiffness of the magnetic bearing. The coupling parameter c_x is 0.5

in theory, but it basically depends on the bearing arrangement [5],[6]. Consequently, it is necessary to compensate these unstable magnetic forces and to apply damping to the system. That means that the minimum demands on the control law are two independent PD position-controllers

$$\mathbf{F}_{PD} = \begin{bmatrix} Px + d_R\dot{x} & Py + d_R\dot{y} \end{bmatrix}^{\mathrm{T}} ,$$

which stabilize the radial deflection in x- and y-axis. Proportional gain P must fulfil

$$P > (1 + c_x)\, k_x$$

to obtain a resulting positive stiffness independent of the angel γ. d_R is referred to as the damping coefficient. Small integral actions are generally part of the feedback path to eliminate the control error and to become independent of static load. However, in the proposed approach integrators are neglected because of their small influence on operation behavior at high rotational speeds. Several further assumptions are made:

- The rotor is a rigid circular disk with the mass m and its centre of mass coincides with the origin of the coordinate system.
- Axial displacement as well as tilting deflection is 0.
- Radial deflections are not influenced by axial forces and tilting moments [4].
- The disk is rotating with constant speed Ω ($\gamma = \Omega t$), thus there is no vibration excitation due to accelerating and decelerating.
- Control-forces (PD-controllers) which act on the rotor can be impressed linear [7].

Additional damping

$$\mathbf{F}_D = \begin{bmatrix} d_a\dot{x} & d_a\dot{y} \end{bmatrix}^{\mathrm{T}}$$

is applied if the rotor is placed in a medium, like for pump applications, with d_a indicating the damping coefficient. Finally, any kind of disturbance is introduced by

$$\mathbf{F}_{EXT} = \begin{bmatrix} F_{x_{EXT}} & F_{y_{EXT}} \end{bmatrix}^{\mathrm{T}} .$$

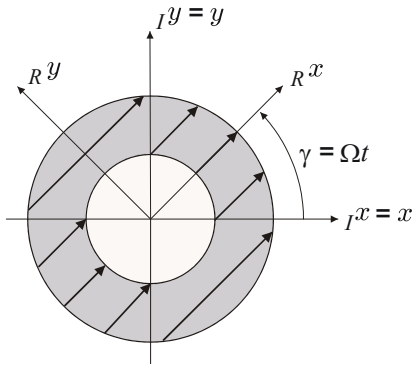

FIGURE 1: (I)nitial and (R)eference coordinates

Equation of Motion

Setting up a mathematical model in stationary coordinates using Newton's law

$$m_I\ddot{\mathbf{y}} = \sum {}_I\mathbf{F} , \tag{1}$$

the equation of motion appears in a non-linear characterisation, which makes it difficult to handle. The two radial coordinates of the centre of mass

$${}_I\mathbf{y} = \begin{bmatrix} {}_Ix & {}_Iy \end{bmatrix}^{\mathrm{T}}$$

are assumed to be in an (I)nitial stationary coordinate system. According to classical rotordynamics books by Gasch, Nordmann and Pfützner [8], and Krämer [9], rotor models of non-circular shafts show the same equation characteristics. It is simpler to transform these two coupled differential equations with periodically time-varying coefficients (1) to a (R)eference coordinate system rotating with angular speed by using the principle of virtual displacement [10]

$$\delta_I\mathbf{y} = \mathbf{T}\delta_R\mathbf{y} \ , \ \mathbf{T} = \begin{bmatrix} \cos(\gamma) & \sin(\gamma) \\ -\sin(\gamma) & \cos(\gamma) \end{bmatrix} . \tag{2}$$

The transformation $\mathbf{T}$ as shown in Figure 1 is well known as Park Transformation in the field of vector control of AC machines. Applying (2), the equation of motion (1) viewed in the rotating frame has constant coefficients. Using additional parameters

$$\begin{aligned} \omega &= \sqrt{\frac{P - k_x}{m}} \\ \varepsilon_k &= \frac{c_x k_x}{P - k_x} = [0, 1] \\ D &= \frac{d_R + d_a}{2m\omega} , \end{aligned} \tag{3}$$

it can be combined to

$$\mathbf{M}_{R}\ddot{\mathbf{y}} + (\mathbf{D}+\mathbf{G})_{R}\dot{\mathbf{y}} + (\mathbf{K}+\mathbf{N})_{R}\mathbf{y} = \frac{1}{m}{}_{R}\mathbf{F}_{EXT} \quad (4)$$

with the mass matrix $\mathbf{M} = \mathbf{M}^{\mathrm{T}}$

$$\mathbf{M} = \begin{bmatrix} 1 & 0 \\ 0 & 1 \end{bmatrix} ,$$

the gyroscopic matrix $\mathbf{G} = -\mathbf{G}^{\mathrm{T}}$ and the damping matrix $\mathbf{D} = \mathbf{D}^{\mathrm{T}}$

$$\mathbf{D}+\mathbf{G} = \begin{bmatrix} 2D\omega & -2\Omega \\ 2\Omega & 2D\omega \end{bmatrix} ,$$

the circulatory matrix $\mathbf{N} = -\mathbf{N}^{\mathrm{T}}$ and the stiffness matrix $\mathbf{K} = \mathbf{K}^{\mathrm{T}}$

$$\mathbf{K}+\mathbf{N} = \begin{bmatrix} (1-\varepsilon_k)\omega^2 - \Omega^2 & -2D\omega\Omega \\ 2D\omega\Omega & (1+\varepsilon_k)\omega^2 - \Omega^2 \end{bmatrix} .$$

ROTORDYNAMIC BEHAVIOR

Natural Frequencies

First, the homogeneous part of the differential equation (4) is solved by neglecting damping. Assuming a solution of the form

$${}_{R}\mathbf{y}_h = \mathbf{y}_v e^{\lambda t}$$

one obtains

$$\left(\lambda^2\mathbf{M} + \lambda\mathbf{G} + \mathbf{K}\right)\mathbf{y}_v = 0 \quad (5)$$

and for $\mathbf{y}_v \neq 0$ the characteristic equation is

$$\lambda^4 + 2(\omega^2+\Omega^2)\lambda^2 + (\omega^2-\Omega^2)^2 - \varepsilon_k^2\omega^4 = 0 .$$

Calculation of eigenvalues shows that a region of rotational speed exists

$$\omega\sqrt{1-\varepsilon_k} < \Omega < \omega\sqrt{1+\varepsilon_k}$$

at which instability occurs. In the stable case, harmonic natural vibrations of frequencies

$${}_{R}\omega_{1,2} = \pm\sqrt{(\omega^2+\Omega^2) - 2\omega\Omega\sqrt{1+\left(\frac{\omega}{2\Omega}\varepsilon_k\right)^2}}$$

and

$${}_{R}\omega_{3,4} = \pm\sqrt{(\omega^2+\Omega^2) + 2\omega\Omega\sqrt{1+\left(\frac{\omega}{2\Omega}\varepsilon_k\right)^2}}$$

arise, which show elliptical mode shapes [11]. However, natural frequencies describe an oscillation behavior in a rotating coordinate system. To achieve the frequencies in a stationary coordinate system, the homogenous solution must be calculated and transformed back to ${}_{I}x$-${}_{I}y$ coordinates. For that, the eigenvectors of (5) can be obtained applying a general approach

$$\mathbf{y}_{v1,2,3,4} = \begin{bmatrix} \lambda_{1,2,3,4}^2 + (1+\varepsilon_k)\omega^2 - \Omega^2 \\ -2\Omega\lambda_{1,2,3,4} \end{bmatrix} .$$

Assuming a stable region of rotational speed, the eigenvalues are $\lambda_{1,2,3,4} = \pm j_R\omega_{1,3}$. Hence, the eigenvectors can be combined to

$$\begin{aligned} \mathbf{y}_{v1} &= \begin{bmatrix} a_{re} \\ jb_{im} \end{bmatrix}, \ \mathbf{y}_{v2} = \mathbf{y}_{v1}^* = \begin{bmatrix} a_{re} \\ -jb_{im} \end{bmatrix} , \\ \mathbf{y}_{v3} &= \begin{bmatrix} c_{re} \\ jd_{im} \end{bmatrix}, \ \mathbf{y}_{v4} = \mathbf{y}_{v3}^* = \begin{bmatrix} c_{re} \\ -jd_{im} \end{bmatrix} , \end{aligned}$$

with the real coefficients a_{re}, b_{im} ,c_{re} and d_{im}. The general solution of the homogeneous equation is

$$\begin{aligned} {}_{R}\mathbf{y}_h = \ & c_1\mathbf{y}_{v1}e^{j_R\omega_1} + c_1^*\mathbf{y}_{v1}^*e^{-j_R\omega_1} \\ & + c_2\mathbf{y}_{v3}e^{j_R\omega_3} + c_2^*\mathbf{y}_{v3}^*e^{-j_R\omega_3} , \end{aligned}$$

whereas $c_1 = c_2 = 1$ is no constraint. Rewriting in real form one gets

$${}_{R}\mathbf{y}_h = \begin{bmatrix} 2a_{re}\cos({}_{R}\omega_1 t) + 2c_{re}\cos({}_{R}\omega_3 t) \\ -2b_{im}\sin({}_{R}\omega_1 t) - 2d_{im}\sin({}_{R}\omega_3 t) \end{bmatrix} . \quad (6)$$

Finally, a back-transformation of (6) results in the natural frequencies

$${}_{I}\omega_{1,2} = \Omega \pm {}_{R}\omega_1 , \quad {}_{I}\omega_{3,4} = \Omega \pm {}_{R}\omega_3 .$$

Figure 2 shows these natural frequencies as a function of rotational speed Ω. Because of back transformation elliptical mode shapes can be seen as general Lissajous-Figures from a stationary coordinate system. Decreasing ε_k leads to the asymptotes

$${}_{I}\omega_{1,2,3,4} \underset{\varepsilon_k\to 0}{=} 2\Omega \pm \omega , \ \pm\omega .$$

Influence of Damping

If damping ratio D is small, the influence of damping on natural frequencies is weak. However, damping of controller and medium is always present and ensures that compared to the undamped case, the

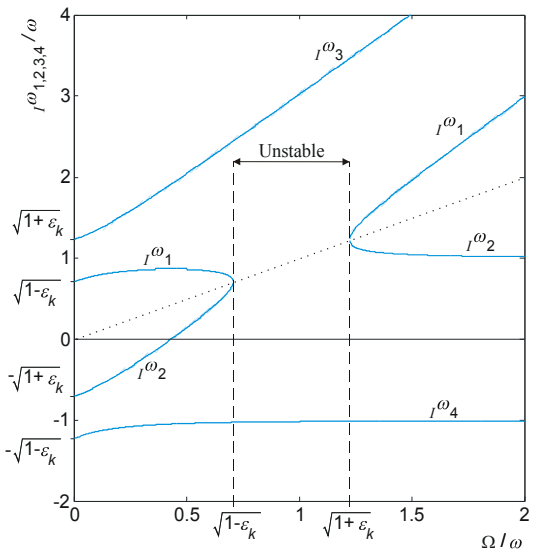

FIGURE 2: Natural frequencies for $\varepsilon_k = 0.5$

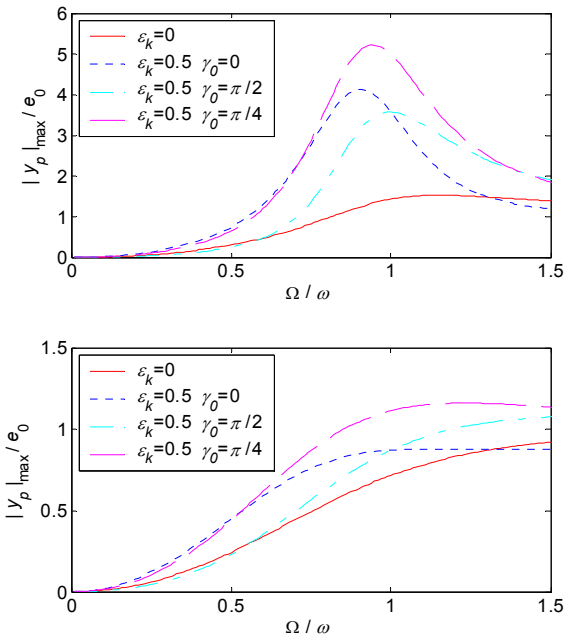

FIGURE 3: Magnitude of displacement for static unbalance for $D = 0.35$ (top) and $D = 0.7$ (bottom)

region of instability reduces and that amplitudes near resonance frequencies remain limited. The influence on stability boundary can be tested by using Routh-Hurwitz Stability Criterion on the characteristic polynomial

$$\det\left(\lambda^2\mathbf{M} + \lambda(\mathbf{D}+\mathbf{G}) + (\mathbf{K}+\mathbf{N})\right) = a_0 + .. + a_4\lambda^4 \ .$$

Instability occurs when coefficient a_0 gets 0. Accordingly, one can find a rotational speed dependent limit of damping ratio

$$D > \frac{1}{2\omega\,|\Omega|}\sqrt{\left|-\left(\omega^2-\Omega^2\right)^2+\varepsilon_k^2\omega^4\right|}$$

for stability. Stability charts are found in [8],[9]. Gaining asymptotical stability over the whole rotational speed range results in a minimum of damping ratio

$$D_{\min}(\varepsilon_k) = \sqrt{\frac{1}{2}\left(1-\sqrt{1-\varepsilon_k^2}\right)} \ . \qquad (7)$$

Static Unbalance

Next, unbalance is introduced, which is the most frequent source of disturbances. A static unbalance arises from the eccentricity e_0 of the centre of gravity from the geometric centre established by the coordinate system [8]. For stationary speed in a rotating coordinate system centrifugal force acts constantly on the rotor with

$$me_0\Omega^2 \begin{bmatrix} \cos(\gamma_0) \\ \sin(\gamma_0) \end{bmatrix} \ .$$

γ_0 describes the polar place of the eccentricity e_0 and it is the angle of the applied centrifugal force. It is assumed that damping ratio is above (7) and thus the homogeneous solution converges to 0. Hence, the constant displacement

$${}_R\mathbf{y}_p = \begin{bmatrix} x_e & y_e \end{bmatrix}^{\mathrm{T}}$$

from the particular solution of (4) leads to

$$\begin{bmatrix} x_e \\ y_e \end{bmatrix} = (\mathbf{K}+\mathbf{N})^{-1} e_0\Omega^2 \begin{bmatrix} \cos(\gamma_0) \\ \sin(\gamma_0) \end{bmatrix} \ .$$

The magnitude of displacement is given by

$$|\mathbf{y}_p|_{\max} = \sqrt{x_e^2+y_e^2} = f(e_0,\Omega,\gamma_0,D,\varepsilon_k) \ . \qquad (8)$$

Figure 3 shows resonance curves for different values of D and ε_k. An interesting aspect is that the maximum deflections as well as the rotational speeds at which the maxima occur are strongly influenced by the angle γ_0. Particulary, $\gamma_0 = \frac{\pi}{4} + n\frac{\pi}{2}$ leads to the highest peaks. However, substituting $\varepsilon_k = 0$ in (8), the magnitude becomes independent of the angle γ_0.

External Disturbances

In concrete applications, radial position control is disturbed by a sum of process forces and self excited

forces. These disturbances can be split up in harmonic terms

$$ {}_R\mathbf{F}_{EXT} = F_{EXT} \begin{bmatrix} \cos(\Omega_E t) \\ \sin(\Omega_E t) \end{bmatrix} \tag{9} $$

to calculate the influence of each part. (9) can be rewritten in

$$ {}_R\mathbf{F}_{EXT} = \mathbf{h}_F + \mathbf{h}_F^* $$

with

$$ \mathbf{h}_F = \frac{F_{EXT}}{2} \begin{bmatrix} 1 \\ -j \end{bmatrix} e^{j\Omega_E t} \ , \ j = \sqrt{-1} $$

to make a solving of the differential equation easier. Applying enough damping, the system shows stability and the partial solution of (4) is given by

$$ \begin{aligned} {}_R\mathbf{y}_{\mathbf{h}_F} &= \left(\Omega_E^2\mathbf{M} + j\Omega_E(\mathbf{D}+\mathbf{G}) + (\mathbf{K}+\mathbf{N})\right)^{-1} \frac{\mathbf{h}_F}{m} \\ &= \begin{bmatrix} x_{re} + jx_{im} \\ y_{re} + jy_{im} \end{bmatrix} e^{j\Omega_E t} \end{aligned} $$

Total solution

$$ \begin{aligned} {}_R\mathbf{y}_p &= {}_R\mathbf{y}_{\mathbf{h}_F} + {}_R\mathbf{y}^*_{\mathbf{h}_F} \\ &= \begin{bmatrix} 2x_{re}\cos(\Omega_E t) - 2x_{im}\sin(\Omega_E t) \\ 2y_{re}\cos(\Omega_E t) - 2y_{im}\sin(\Omega_E t) \end{bmatrix} \end{aligned} $$

can be combined to

$$ \begin{aligned} {}_R\mathbf{y}_p = &(x_{re} - y_{im})\,\mathbf{r}_v(\Omega_E) \\ &+ (y_{re} + x_{im})\,\mathbf{r}_v(\Omega_E + \frac{\pi}{2}) \\ &+ (x_{re} + y_{im})\,\mathbf{r}_v(-\Omega_E) \\ &+ (y_{re} - x_{im})\,\mathbf{r}_v(-\Omega_E + \frac{\pi}{2}) \end{aligned} $$

with the vector

$$ {}_R\mathbf{r}_v(\Omega_E) = \begin{bmatrix} \cos(\Omega_E t) & \sin(\Omega_E t) \end{bmatrix}^{\mathrm{T}} $$

as a unit circle movement. The steady state solution contains two positive and two negative rotating orbits, except for $\Omega_E = 0$, but this case is almost the same as that mentioned in the previous section. If only the maximum radial amplitude of deflection is important, it can be calculated by

$$ \begin{aligned} |\mathbf{y}_p|_{\max} = &\sqrt{(x_{re} - y_{im})^2 + (y_{re} + x_{im})^2} \\ &+ \sqrt{(x_{re} + y_{im})^2 + (y_{re} - x_{im})^2} \ . \end{aligned} $$

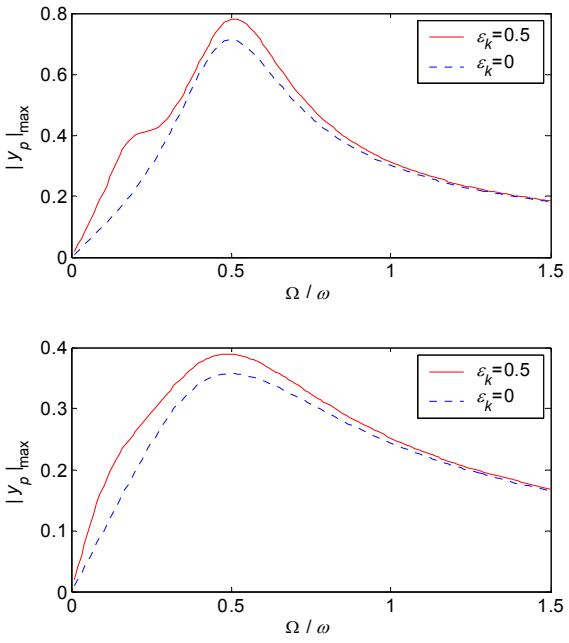

FIGURE 4: Maximum radial deflection applying ${}_I\mathbf{F}_{EXT} = c_E\Omega \begin{bmatrix} \cos(2\Omega t) & \sin(-2\Omega t) \end{bmatrix}^{\mathrm{T}}$ for $D = 0.35$ (top) and $D = 0.7$ (bottom)

As an example, Figure 4 shows maximum radial deflection for

$$ {}_I\mathbf{F}_{EXT} = c_E\Omega \begin{bmatrix} \cos(2\Omega t) & \sin(-2\Omega t) \end{bmatrix}^{\mathrm{T}} $$

as source of disturbance. It shall only give a quantitative overview of the influence of ε_k and damping ratio D, wherefore y-axis scaling is not specified in detail.

DISCUSSION OF RESULTS

Figure 3 and 4 illustrate the influence of ε_k and D on the resonance curves. As seen in (3), increasing proportional gain P of controllers leads to a smaller ε_k and therefore to an improved operation behavior. Another point is that a small ε_k only needs a small damping ratio D to achieve global stability. However, high controller gains are only supported by expansive power electronics. Moreover, applying a high damping ratio D (controller and surrounding fluids), ε_k loses influence on the closed loop control. Increasing D by the controller, though, the noise of the position sensors gains influence too.

The outcome is that resonance phenomena follow from controller settings with low gain and low damping ratio, which one should pay attention to.

On the other hand, high gain and high damping ratio (surrounding fluids) add up to a stationary behavior where non-linearity of the plant loses influence on the closed-loop control and applying a simple linear control is sufficient effort for the requirements of many applications. Non-linear controller design methods are able to ensure $\varepsilon_k = 0$ without using high gain or high damping ratio and for applications, where the rotor is placed in air (small damping ratio), complex control strategies can yield to a much better operation performance.

CONCLUSION

In this paper rotordynamic aspects of a bearingless slice motor have been introduced. Resonance phenomena as well as the consequence of applying disturbance forces are derived from a mathematical model and should give engineers an overview of possible problems by neglecting non-linear parts of the plant to be controlled.

ACKNOWLEDGEMENTS

The research works on improvements of bearingless motors are realized in projects of the 'Linz Center of Competence in Mechatronics' as a part of the Kplus-program of the Austrian government. The presented project is kindly supported by Levitronix GmbH Zürich, the Austrian and Upper Austrian government and the Johannes Kepler University of Linz. The authors thank all involved partners for their support.

REFERENCE

1. M. Neff, N. Barletta, R. Schöb: *Bearingless Centrifugal Pump for Highly Pure Chemicals*, Proc. of the 8th Int. Symp. on Magnetic Bearings, Mito, 2002.

2. S. Ueno, C. Chen, T. Ohishi, K. Matsuda, Y. Okada, Y. Taenaka, T. Masuzawa: *Design of a Self-Bearing Slice Motor for a Centrifugal Blood Pump,* Proc. of the Power Conversion Intelligent Motion, Nürnberg, 1998.

3. R. Schöb, N. Barletta: *Principle and Application of a Bearingless Slice Motor*, Proc. of the 5th Int. Symp. on Magnetic Bearings, Kanazawa, 1996.

4. K. Nenninger, W. Amrhein, S. Silber, G. Trauner. M. Reisinger: *Magnetic Circuit Design of a Bearingless Single-Phase Slice Motor*, Proc. of the 8th Int. Symp. on Magnetic Bearings, Mito, 2002.

5. Ch. Hüttner: *Regelungskonzepte magnetisch gelagerter Scheibenmotoren*, Dissertation, ETH Zürich Nr. 15092, 2003.

6. Ch. Hüttner: *Nonlinear State Control of a Left Ventricular Assist Device*, Proc. of the 8th Int. Symp. on Magnetic Bearings, Mito, 2002.

7. S. Silber: *Beiträge zum lagerlosen Einphasenmotor*, Dissertation, Institut für Regelungstechnik und elektrische Antriebe, J. K. Universität Linz, 2000

8. R. Gasch, R. Nordmann, H. Pfützner: *Rotordynamik*, 2. Auflage, Springer, 2001.

9. E. Krämer: *Dynamics of Rotors and Foundations*, Springer, 1993.

10. H. Bremer: *Dynamik und Regelung mechanischer Systeme*, B. G. Teubner Stuttgart, 1988.

11. E. Steinhardt, G. Schweitzer: *Gleich und Gegenlauf bei der unsymmetrischen Lavalwelle*, ZAMM 57, T90 - T92, 1977.